3-d Models for Hyperbolic Tessellation

JOSH INOUE

September 25, 2014

Abstract

Hyperbolic space can be tessellated in many intricate and fascinating ways. Firstly we want to take an interesting element of one tessellation and build a Euclidian 3-d model that demonstrates its symmetries. Next we find an economical way of printing it using the 3-d printer, which keeps its structural integrity. Finally once we have got the models, Dan Yasaki experimentally showed these tessellations can be constructed by using only eight types of smaller "building blocks", in different numbers and arrangements. The plan is to create a puzzle using that idea allowing the structure and symmetry to be explored.

Acknowledgements

I would like to thank my supervisor, Dr Herbert Gangl, for his enthusiasm and continued support throughout this project. I hope he is as excited about my models as I am. I would also like to pay tribute to Beth and Richard for their help and invaluable advice and guidance with the 3-d printer. It couldn't have been done without their willingness to get involved . Finally to BP for providing this opportunity to venture into the curved world of hyperbolic space and emerge with more questions than at the start.

1 Introduction

1.1 Hyperbolic Space

Around 300 B.C. Euclid wanted formalise and collate the geometry of the day in one place. In his work called the "Elements" he had five axioms from which he proved many theorems and built up the geometry which today is known as Euclidean geometry. However his fifth axiom seem to many to be unnecessary, and over the years mathematicians tried to deduce the fifth from the other four. Through this Hyperbolic Geometry was discovered.

Today we can express the fifth axiom as, *"Through any point not lying on a straight line there exists one and only one straight line that does not intersect the first."* If we replace *one and only one* by *at least two* this forms the basis to this new geometry. We will visualise this space mostly in this paper by the Upper-Half Plane Model (UHP), with points in Hyperbolic 2-Space denoted by, $\mathbb{H}^2 := \{x + iy \mid y > 0; x, y \in \mathbb{R}\}$ and the Upper-Half Space Model, with points in Hyperbolic 3-Space denoted by $\mathbb{H}^3 := \{z + jw \mid w > 0; w \in \mathbb{R}, z \in \mathbb{C}\}$. Here $\mathbb{H}^3$ is a subset of points from the Quaternions, denoted $\mathbb{H}$.

In Hyperbolic space the shortest lines between two points are arcs of half circles centre on the real axis and vertical lines perpendicular to the real line, and planes are half spheres centred on the complex plane and vertical planes perpendicular to the complex plane. We take the boundary to be the real line in $\mathbb{H}^2$ and the complex plane in $\mathbb{H}^3$ both with the point at infinity, i.e. $\partial\mathbb{H}^2 = \mathbb{R} \cup \{\infty\}$, and $\partial\mathbb{H}^3 = \mathbb{C} \cup \{\infty\}$.

1.2 Fundamental Domains

If we consider a Möbius Transformation, $z \mapsto \frac{az+b}{cz+d}$, that maps the UHP to the UHP, we will have real a, b, c and d. Möbius transformations of this type also have the property that they are conformal maps, hence with the added condition that $ad - bc = 1$, any isometry of $\mathbb{H}^2$ can be represented by the matrix $A = \left(\begin{smallmatrix} a & b \\ c & d \end{smallmatrix}\right)$ with $det(A) = 1$, i.e. $A \in SL_2(\mathbb{R})$, where an *isometry* is a map from one metric space to another that preserves the distance between points in the respective metric.

Now if we take the map that translates along the real line, $\left(\begin{smallmatrix} 1 & 1 \\ 0 & 1 \end{smallmatrix}\right)$ equivalent to $z \mapsto z + 1$; and the reflected inversion map, $\left(\begin{smallmatrix} 0 & -1 \\ 1 & 0 \end{smallmatrix}\right)$ equivalent to $z \mapsto -\frac{1}{z}$, then denote the group generated by these two elements, $\Gamma \subseteq SL_2(\mathbb{Z})$ we have an infinite group that is "arithmetic", which without going into detail is important in producing tessellation which cover the whole space [2].

We also need to be familiar with the concept of group actions: An action of a group G on a set X is a function,

$$\begin{array}{rccc} \varphi: & X \times G & \to & X \\ & (x, g) & \mapsto & \varphi(x, g) \end{array}$$

with the properties that,

$$\begin{array}{lrcll} (1) & \varphi(\varphi(x, g), h) & = & \varphi(x, gh) & \forall\, x \in X;\, g,\, h \in G \quad \text{[Closure]} \\ (2) & \varphi(x, e) & = & x & \forall\, x \in X; e \text{ identity of } G \quad \text{[Identity]} \end{array}$$

This can be also viewed as a group homomorphism $\varphi : G \to S_X$, S_X the symmetric group on X and $\varphi(g)$ assigned a permutation such that $\varphi(g)\varphi(h) = \varphi(gh)$.

If we take our Hyperbolic 2-Space and the group Γ, then the group action of Γ on a single element z of our space produce many images of that element called the Γ-orbit of the action on z. A fundamental domain for the action of Γ is defined as a set of points which contains exactly one element from each of these Γ-orbits for all z in our space, $\mathbb{H}^2$.

For this Γ if we take the subset, $\{z \in \mathbb{H}^2 : |z| > 1,\ |\mathrm{Re}(z)| < \frac{1}{2}\}$ with the boundary on one side and half the arc at the bottom, this is a fundamental domain for the action of $\Gamma = \langle \left(\begin{smallmatrix} 1 & 1 \\ 0 & 1 \end{smallmatrix}\right),\ \left(\begin{smallmatrix} 0 & -1 \\ 1 & 0 \end{smallmatrix}\right) \rangle$ on $\mathbb{H}^2$. Each cell in [Fig. 1] represents a Γ translate of the fundamental domain.

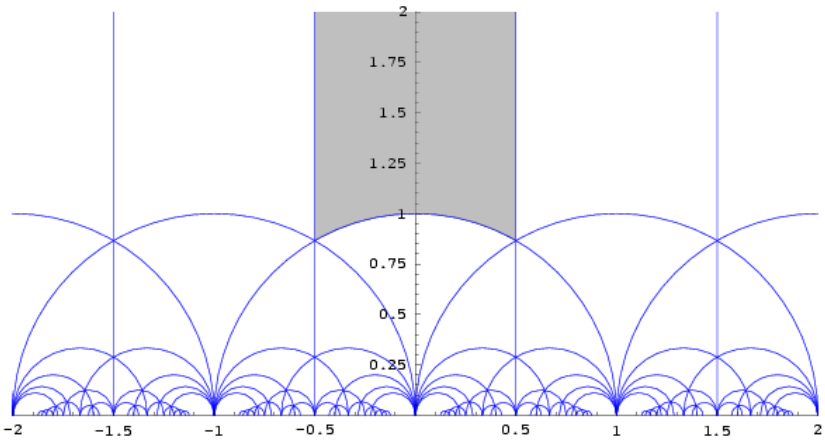

Figure 1: The fundamental domain for the action of Γ on $\mathbb{H}^2$ [source: Wikipedia]

This notion leads us to the idea of a tessellation, by finding a fundamental domain, all the isometric translates of it will cover the whole of the space, hence will be our tessellation for the space. We are not too concerned about restricting which points are included at the boundary of the fundamental domain, so we include all of them. This means there will be a slight overlap when we apply the Γ translates, but that will not matter in finding our tessellation.

Moving to Hyperbolic 3-Space, our isometries of $\mathbb{H}^3$ are represented by elements of the group $SL_2(\mathbb{C})$, and it is here where we search for subgroups, $\Gamma \subseteq SL_2(\mathbb{C})$ that act on $\mathbb{H}^3$ to produce fundamental domains from which we can take a union to form interesting tessellations.

1.3 The Tessellations of $\mathbb{H}^3$

Take the imaginary quadratic number field $K = \mathbb{Q}(\sqrt{-d})$, with $d > 0$ a square-free integer and d_K the discriminant of K and $\mathcal{O}_K$ the ring of integers in K. Then $\mathcal{O}_K$ has a $\mathbb{Z}$-basis, $\{1, \theta\}$, with

$$\theta = \begin{cases} \frac{1+\sqrt{-d}}{2} & -d \equiv 1 \bmod 4, \\ \sqrt{-d} & -d \equiv 2, 3 \bmod 4. \end{cases}$$

For each d, we obtain the tessellation from points in $\mathbb{Z}[\theta] \subseteq \mathbb{C}$ of the form,

$$\left\{ \frac{x}{z-w},\ \frac{y}{z-w} \cdot \theta \right\} \in SL_2(\mathbb{Z}[\theta]) \tag{1}$$

There is a Γ-equivariant bijection between those points that form the boundary of the fundamental domain and a particular set of integer solutions to,

$$Q_d(x,\ y,\ z,\ w) = x^2 + d \cdot y^2 + z^2 - w^2 \tag{2}$$

Here our solution set has the added condition that the z and w component must have the same parity (odd/even), with the GCD of the four components equal to one, except when the z and w components have opposite parity when you multiply all the entries by two. This will give us finitely many points and our bijection [1].

Thus we have a way of generating fundamental domains for any d. For example $d = 1$ we are looking a fundamental domain corresponding to the group $SL_2(\mathbb{Z}[i])$, with $\mathbb{Z}[i]$ the Gaussian integers. It turns out that if we glue together four copies of our fundamental domain, i.e. take a union, we obtain an Octahedron which represents a tessellation of our space [Fig. 2].

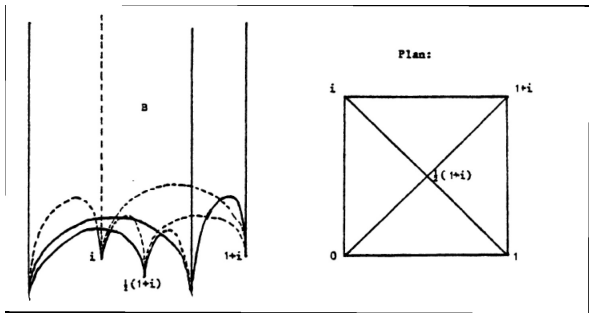

Figure 2: Tessellation of $\mathbb{H}^3$ with $d = 1$ [Source: J. Cremona, Comp. Math. 51, no.3 (1984) [3]]

For $d = 2$ our group is now $SL_2(\mathbb{Z}[\sqrt{-2}])$ and the corresponding union of fundamental domains to obtain our tessellating polytope is show in [Fig.3].

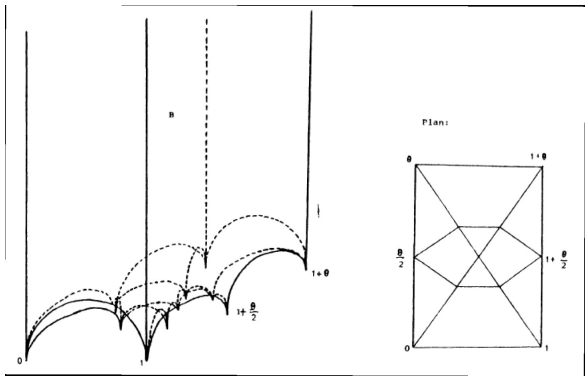

Figure 3: Tessellation of $\mathbb{H}^3$ with $d = 2$ [Source: J. Cremona, Comp. Math. 51, no.3 (1984) [3]]

Going back to our model for hyperbolic space (Upper-Half Space Model) we can interpret the diagrams on the left as the intersection of 4 and 10 half-spheres respectively and 4 vertical planes that correspond to the faces on out tessellating polytope. [Fig. 4] is a representation of these half spheres. The diagrams on the right are projections of the polytope from the point at infinity. Note that the vertices of these polytopes are all on the boundary, $\partial\mathbb{H}^3$ and are of the form in (1).

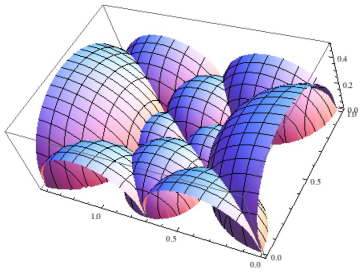

Figure 4: Another view of the fundamental domain for $d = 2$ [using Mathematica] [2]

Thus our first glimpse at what these polytopes look like can be visualised by bringing the point at infinity down as in [Fig. 5].

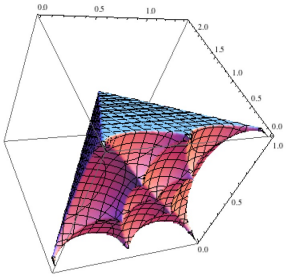

Figure 5: A tangible representation of the fundamental domain for $d = 2$ [using Mathematica] [2]

I already have a comprehensive list of the points needed to form these fundamental domains for d up to 696 [9] in the form of integer solutions to (2) as a list of vertices coordinates and vectors for the vertices that make up each face and edge for all of the polytopes needed to tessellate the space for every d. My starting point is to find a way to "spherify" these fundamental domains in a way that preserves their symmetry.

2 Creating the Polytopes

2.1 Initial Thoughts

To immediately get from the four dimensional points generated by (2) to three we just remove one of the coordinates, say the last, and plot the resulting points. We get a shape which is skewed off in one direction, as demonstrated by Matthew Spencer in his 2012 summer project. Removing the other coordinates in turn gives the same basic shape except they are skewed in a different way [Fig. 6]. From observation, removing the last coordinate gives the least skewed polytope.

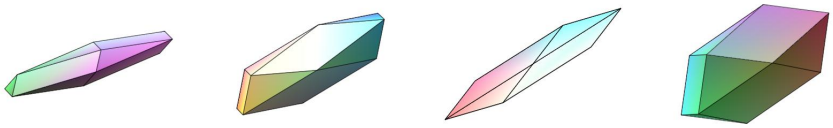

Figure 6: 1^{st}, 2^{nd}, 3^{rd} and 4^{th} coordinate removed respectively for $d = 2$ [using Maple]

To find the a way of getting a non skewed polytope I consider a linear transformation that takes the 4-dimensional points and outputs 3-dimensional points that lie on a sphere.

2.2 The Transformation

We first go back to considing equation (2) that generates the vertices of our polytopes,

$$x^2 + d \cdot y^2 + z^2 - w^2 = 0$$

A set of solutions that are invariant of d occur when the y component is 0. These are {0, 0, 1, 1}, {0, 0, -1, 1} and {-2, 0, 0, 2}, where the solution is denoted by {*x, y, z, w*}. Let us assume that these points are actually from an equilateral triangle side length 2 and thus we can map them to the points {0, 0, 1}, {0, 0, -1} and {$-\sqrt{3}$, 0, 0} respectively. This with a fourth point will uniquely define a transformation from 4-d to 3-d.

2.3 Classes of Polytope and Initial Results

The first polytopes found for each d can be classified into at least four types. If we look at their underlying symmetry group or the stabiliser of the polytope we can group them into ones isomorphic to the Octahedron/Cube [$C_2 \times S_4$], the Tetrahedron [S_4], the Triangular Prism [$C_2 \times D_3$] and the Hexagonal Cap [D_3].

2.3.1 Octahedral symmetry, $[C_2 \times S_4]$

For d satisfying the relation,

$$3d - 2 = n^2;\ n,\ d \in \mathbb{Z} \tag{3}$$

We have another triple of points that will always be included in our union of fundamental domains as they satisfy the conditions in (2), namely

$$\begin{array}{llll} \{-2d, & 2\sqrt{3d-2}, & 1, & 4d-1\}, \\ \{-2d, & 2\sqrt{3d-2}, & -1, & 4d-1\}, \\ \{-2d+2, & 2\sqrt{3d-2}, & 0, & 4d-2\}. \end{array}$$

This gives another triangle that is opposite the first one pointing in the other direction. Hence if we map it so the two centres align and the vertices lie on a sphere we will obtain our un-skewed shape for these cases. It turns out that the most interesting and complex polytopes are of this form, with $d = \frac{n^2+2}{3}$. This then already allows us to form a whole family of polytopes as they will all contain the triple of points described above. The linear transformation for this class is then,

$$L: \begin{array}{c} x \\ y \\ z \\ w \end{array} \mapsto \begin{array}{l} \frac{\sqrt{3}}{2} \cdot x \\ \frac{\sqrt{6}}{3} \cdot y \\ z \end{array} + \frac{\sqrt{3d-2}}{6} \cdot \sqrt{3} \cdot y \tag{4}$$

It turns out that the w is not needed in the linear transformation, and that our first guess that removing the last coordinate was a step in the right direction. Note this does not centre the polytope on the origin and a translation of $\frac{\sqrt{3}}{3}$ along the $x-$axis and Y_t along the $y-$ axis is required to move the vertices onto a sphere, radius r centred on the origin, which is included below.

d	1	2	6	9	17	22	34	...	$\frac{n^2+2}{3}$
$\sqrt{3d-2}$	1	2	4	5	7	8	10	...	n
r	$\sqrt{2}$	2	$2\sqrt{3}$	$3\sqrt{2}$	$\sqrt{34}$	$2\sqrt{11}$	$2\sqrt{17}$	...	$\sqrt{2d}$

Table 1: Values relating to (4)

2.3.2 Tetrahedra and Octahedra

For d of the form, $d = 3n^2$ we obtain a Tetrahedron, and for $d = 3n^2 - 2$ we obtain an Octahedron for the first polytopes in the list for each d.

2.3.3 Triangular Prism symmetry, $[C_2 \times D_3]$

More interestingly, if we take d of the form $d = 3n^2 + \frac{4}{\alpha} \cdot n$ with $\frac{4}{\alpha} \cdot n,\ \alpha \in \mathbb{N}$ then what we get are structures that have symmetry isomorphic to that of the

triangular prism. These polytopes have the triple of points which again satisfy the conditions in (2) for all valid d,

$$\begin{array}{llll} \{-\alpha n, & \alpha, & 1, & 2\alpha n+1\}, \\ \{-\alpha n, & \alpha, & -1, & 2\alpha n+1\}, \\ \{-\alpha n-2, & \alpha, & 0, & 2\alpha n+2\}. \end{array}$$

This produces another equilateral triangle opposite the first, oriented in the same way. Like above this can be used to calculate the transformation for this class, which in this case is non-unique as the triangular prism can have different length sides to its triangular faces. If we impose the condition that the points lie on a sphere then indeed our transformation is unique, and it is these results I have calculated in what follows. (5) is the general transformation for this class with the first few values for K, n, and d for each α in Table 2.

$$L: \begin{array}{c} x \\ y \\ z \\ w \end{array} \mapsto \begin{array}{c} \frac{\sqrt{3}}{2}\cdot x \\ K\cdot y \\ z \end{array} + \begin{array}{c} \frac{n\sqrt{3}}{2}\cdot y \end{array} + \begin{array}{c} \frac{\sqrt{3}}{3} \\ \alpha\cdot\frac{K}{2} \end{array} \tag{5}$$

α	1					2			3		
K	2	2	2	2	2	1	1	1	2	$2\sqrt{3}$	$2\sqrt{5}$
n	1	2	3	4	5	1	3	5	3	9	15
d	7	20	39	64	95	5	33	85	31	225	695

α	4				5	6	8		10
K	$\sqrt{2}$	$\sqrt{6}$	$\sqrt{10}$	$\sqrt{14}$	-	$\sqrt{2}$	1	-	-
n	2	6	10	14	5	3	2	4	3
d	14	114	310	602	79	29	13	50	77

Table 2: Some data for first few α

2.4 Results

For general d the transformation the maps the 4-d points $\{x,\ y,\ z,\ w\}$ to a sphere radius r, centred on the origin is as follows:

$$T: \begin{array}{c} x \\ y \\ z \\ w \end{array} \mapsto \begin{array}{c} \frac{\sqrt{3}}{2}\cdot x \\ K\cdot y \\ z \end{array} + \begin{array}{c} k\cdot y \end{array} + \begin{array}{c} \frac{\sqrt{3}}{3} \\ Y_t \end{array} \tag{6}$$

Table 3 gives the values of k, K, Y_t and r which are valid for all d of the form listed, and Table 4 gives the values for a few α where $m \in \mathbb{N}$. In Table 5 find the data for the first polytopes for each d up to $d = 34$ for the transformation in (6).

Class	d	k	K	Y_t	r
Octahedral	$\frac{n^2+2}{3}$	$\sqrt{3d-2}\cdot\frac{\sqrt{3}}{6}$	$\frac{\sqrt{6}}{3}$	$-\sqrt{3d-2}\cdot\frac{\sqrt{6}}{3}$	$\sqrt{2d}$
Triangular Prism	$3n^2+\frac{4}{\alpha}\cdot n$	$\frac{n\sqrt{3}}{2}$	K_α	$\alpha\cdot\frac{K_\alpha}{2}$	r_α
Tetrahedron	$3n^2$	$\sqrt{3d}\cdot\frac{\sqrt{3}}{6}$	$\frac{2\sqrt{6}}{3}$	$-\frac{\sqrt{6}}{6}$	$\frac{\sqrt{6}}{2}$
Octahedron	$3n^2-2$	$\frac{d}{\sqrt{d+2}}\cdot\frac{\sqrt{3}}{6}$	$\frac{2\sqrt{6}}{3}$	$\frac{\sqrt{3}}{\sqrt{d+2}}\cdot\frac{\sqrt{6}}{3}$	$\sqrt{2}$

Table 3: General Transformations

α	n	K_α	r_α
1	m	2	$\frac{\sqrt{21}}{2}$
3	$6m-3$	$2\sqrt{\frac{n}{3}}$	$\sqrt{\frac{d}{n}}$
4	$4m-2$	$\sqrt{n}$	$2\sqrt{\frac{d}{n}}$

Table 4: Values for $\alpha \leq 4$

2.5 Final Thoughts on Theory

There are still a few cases that I haven't been able to classify so a complete list of the transformations would have to be calculated by hand. Also I have only comprehensively looked into values of α up to four, but I have used larger α and calculated the K_α for those cases individually, e.g. for $\alpha = 10,\ n = 10 : d = 304,\ K_\alpha = 2$ Note that I have used data that includes square d and $d \equiv 0 \bmod 4$, although this is not a proper representation of our quadratic number field K it helped in finding the patterns and structures presented above. There is an underlying relation between d and $4d$ that produced the same first polytope, for example d of the form $\frac{n^2+2}{3}$, $4d$ is the same with its transformation given by $-2k$, $K = \frac{2\sqrt{6}}{3}$ and $-Y_t$, where k and $-Y_t$ are the entries for the corresponding d. Also the is a change in sign between these two cases for k and Y_t, this doesn't change anything just represents a slightly different fundamental domain but the end result is the same and the minus signs that occur on the y component can be dropped (as may have been done in some of the generalised transformations above for ease of presentation).

I also looked at the normal vectors to the set of solutions in our 4-d space, as they lie in a supporting hyperplane. For the case where $d = \frac{n^2+2}{3}$ the normal is given by $\{1, -\sqrt{3d-2}, 0, 2\}$. It is thought these hyperplanes for each d is of the form $\{1, *, 0, 2\}$, where * denotes half-integers [1].

d	Stabiliser	Vertices	Class	k	K	Y_t	r
1	$C_2 \times S_4$	6	Octahedral	$\frac{\sqrt{3}}{6}$	$\frac{\sqrt{6}}{3}$	$-\frac{\sqrt{6}}{3}$	$\sqrt{2}$
2	$C_2 \times S_4$	12	Octahedral	$\frac{\sqrt{3}}{6}$	$\frac{2\sqrt{6}}{3}$	$-\frac{2\sqrt{6}}{3}$	2
3	S_4	6	Triangular Prism	$-\frac{\sqrt{3}}{6}$	$\frac{2\sqrt{6}}{3}$	$\frac{\sqrt{6}}{6}$	$\frac{\sqrt{6}}{2}$
4	$C_2 \times S_4$	6	Octahedral	$-\frac{2\sqrt{3}}{6}$	$\frac{2\sqrt{6}}{3}$	$\frac{\sqrt{6}}{3}$	$\sqrt{2}$
5	$C_2 \times D_3$	6	Triangular Prism	$\frac{\sqrt{3}}{2}$	1	-1	$\frac{\sqrt{21}}{3}$
6	$C_2 \times S_4$	24	Octahedral	$\frac{4\sqrt{3}}{6}$	$\frac{\sqrt{6}}{3}$	$-\frac{4\sqrt{6}}{3}$	$2\sqrt{3}$
7	$C_2 \times D_3$	6	Triangular Prism	$\frac{\sqrt{3}}{2}$	2	-1	$\frac{\sqrt{21}}{3}$
8	$C_2 \times S_4$	12	Octahedral	$-\frac{2\sqrt{3}}{3}$	$\frac{2\sqrt{6}}{3}$	$-\frac{2\sqrt{6}}{3}$	2
9	$C_2 \times S_4$	30	Octahedral	$\frac{5\sqrt{3}}{6}$	$\frac{\sqrt{6}}{3}$	$-\frac{5\sqrt{6}}{3}$	$3\sqrt{2}$
10	$C_2 \times S_4$	6	Octahedral	$\frac{5\sqrt{3}}{6}$	$\frac{\sqrt{6}}{6}$	$-\frac{\sqrt{6}}{3}$	$\sqrt{2}$
11	S_4	12	Tetrahedral	$\frac{5\sqrt{3}}{6}$	$\frac{2\sqrt{6}}{3}$	$-\frac{5\sqrt{6}}{6}$	$\frac{\sqrt{22}}{2}$
12	S_4	4	Tetrahedral	$-\frac{2\sqrt{3}}{3}$	$\frac{2\sqrt{6}}{3}$	$\frac{\sqrt{6}}{6}$	$\frac{\sqrt{6}}{2}$
13	$C_2 \times D_3$	12	Triangular Prism	$\sqrt{3}$	1	-4	$\frac{2\sqrt{39}}{3}$
14	$C_2 \times D_3$	12	Triangular Prism	$\sqrt{3}$	$\sqrt{2}$	$-2\sqrt{2}$	$\frac{2\sqrt{21}}{3}$
15	$C_2 \times S_4$	6	Octahedral	$\frac{5\sqrt{3}}{6}$	$\frac{2\sqrt{6}}{3}$	$-\frac{\sqrt{6}}{3}$	$\sqrt{2}$
16	$C_2 \times D_3$	6	Triangular Prism	$-\sqrt{3}$	2	2	$\frac{4\sqrt{3}}{3}$
17	$C_2 \times S_4$	48	Octahedral	$\frac{7\sqrt{3}}{6}$	$\frac{\sqrt{6}}{3}$	$-\frac{7\sqrt{6}}{3}$	$\sqrt{34}$
18	D_3	9	Hexagonal Cap	$\frac{7\sqrt{3}}{6}$	$\frac{\sqrt{6}}{3}$	$-\frac{4\sqrt{6}}{3}$	$2\sqrt{3}$
19	S_4	12	Tetrahedral	$\frac{7\sqrt{3}}{6}$	$\frac{2\sqrt{6}}{3}$	$-\frac{7\sqrt{6}}{6}$	$\frac{\sqrt{38}}{2}$
20	$C_2 \times D_3$	6	Triangular Prism	$-\sqrt{3}$	2	1	$\frac{\sqrt{21}}{3}$
21	$C_2 \times S_4$	6	Octahedral	$\frac{7\sqrt{3}}{6}$	$\frac{\sqrt{6}}{3}$	$-\frac{\sqrt{6}}{3}$	$\sqrt{2}$
22	$C_2 \times S_4$	24	Octahedral	$\frac{4\sqrt{3}}{3}$	$\frac{\sqrt{6}}{3}$	$-\frac{8\sqrt{6}}{3}$	$2\sqrt{11}$
23	D_3	9	Hexagonal Cap	$\frac{7\sqrt{3}}{6}$	$\frac{2\sqrt{6}}{3}$	$-\frac{2\sqrt{6}}{3}$	2
24	$C_2 \times S_4$	24	Octahedral	$-\frac{4\sqrt{3}}{3}$	$\frac{2\sqrt{6}}{3}$	$\frac{4\sqrt{6}}{3}$	$2\sqrt{3}$
25	$C_2 \times S_4$	6	Octahedral	$\frac{25\sqrt{3}}{18}$	$\frac{\sqrt{6}}{9}$	$-\frac{\sqrt{6}}{3}$	$\sqrt{2}$
26	D_3	9	Hexagonal Cap	$\frac{4\sqrt{3}}{3}$	$\frac{\sqrt{6}}{3}$	$-\frac{2\sqrt{6}}{3}$	2
27	S_4	4	Tetrahedral	$\frac{7\sqrt{3}}{6}$	$\frac{2\sqrt{6}}{3}$	$-\frac{\sqrt{6}}{6}$	$\frac{\sqrt{6}}{2}$
28	D_3	6	Hexagonal Cap	$-\frac{4\sqrt{3}}{3}$	$\sqrt{6}$	$\frac{5\sqrt{6}}{6}$	$\frac{\sqrt{22}}{2}$
29	$C_2 \times D_3$	18	Triangular Prism	$\frac{3\sqrt{3}}{2}$	$\sqrt{2}$	$-3\sqrt{2}$	$\frac{\sqrt{174}}{3}$
30	$C_2 \times D_3$	6	Triangular Prism	$\frac{3\sqrt{3}}{2}$	$\frac{1}{2}$	-1	$\frac{\sqrt{21}}{3}$
31	$C_2 \times D_3$	18	Triangular Prism	$\frac{3\sqrt{3}}{2}$	2	-3	$\frac{\sqrt{93}}{3}$
32	$C_2 \times S_4$	6	Octahedral	$-\frac{4\sqrt{3}}{3}$	$\frac{2\sqrt{6}}{3}$	$\frac{\sqrt{6}}{3}$	$\sqrt{2}$
33	$C_2 \times D_3$	6	Triangular Prism	$\frac{3\sqrt{3}}{2}$	1	-1	$\frac{\sqrt{21}}{3}$
34	$C_2 \times S_4$	48	Octahedral	$\frac{5\sqrt{3}}{3}$	$\frac{\sqrt{6}}{3}$	$-\frac{10\sqrt{6}}{3}$	$2\sqrt{17}$

Table 5: Data for First Polytopes with $d \leq 34$

3 3-d Printing

3.1 Software

I have mostly looked at free open source software to build the models. OpenSCAD [5] was found to be particularly useful and was predominantly used to export the polytopes in the .stl formal that can be imported into the 3-d printers software. A invaluable module for OpenSCAD written by Kit Wallace and downloaded from his home page [6] allowed me to input the vertices as vectors, faces as vectors of the vertices in each one and edges as vectors of each end vertex. All of this data was taken from the files created by another Durham student two years previously. With the module it will place cylinders along each edge and spheres at each vertex so creating a wire-frame is very simple from the list of transformed points. Exporting with some of the models can take over an hour if not more for the larger models in particular.

3.2 3-d Printers

After looking at all available options for 3-d printing, I have been working with a powder bed and Ink jet head 3-d printer, the ZPrinter® 650. For this project in particular, the way the models are printed means that no support structure needs to be put in place during printing. With other types of 3-d printer, such as Fused Deposition Modeling (FDM), these models would collapse when trying to print convex polytopes such as the ones we are dealing with.

Figure 7: 3D Systems ZPrinter® 650

The powder bed printer works by laying a layer of starch powder in the printing chamber and an ink-jet printing head fires droplets of coloured binder onto the points in each layer that are to be printed. This process repeats and can take over 10 hours from some of the models. Once the printer has finished, the models need to be 'excavated'. This just means we need to remove the excess powder from the print chamber that hasn't solidified which can then be reused in another print. We do this by vacuuming it up very carefully, trying not to disturb our models as although they are solid they are still very fragile, and can easily break. If we try to remove the hollow structure with powder still inside it can cause the whole thing to fall apart under the weight of the excess powder so consideration into the design of the polytopes must be taken into account when printing them with this method.

Figure 8: Models of different thickness for $d = 19$ being "excavated"

Once removed from the printer the models are then cleaned. The left over powder still stuck on can be blown off using one of the fine tools in the printers processing chamber. The models then need to be glued using cyanoacrylate, a strong fast acting adhesive. This process involves pouring the adhesive over the model and allowing it to soak in. It is a slightly exothermic reaction and solidifies the whole model completely.

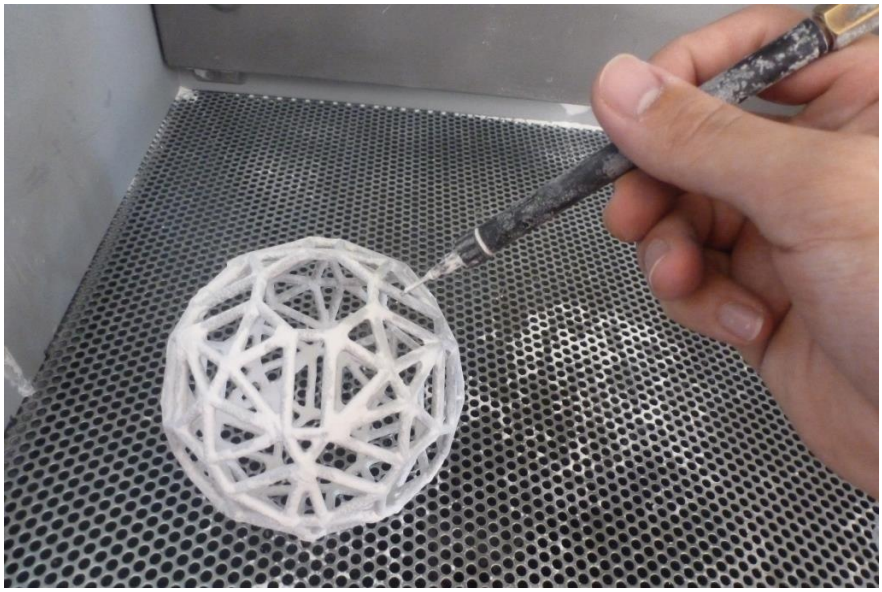

Figure 9: Models for $d = 41$ being cleaned

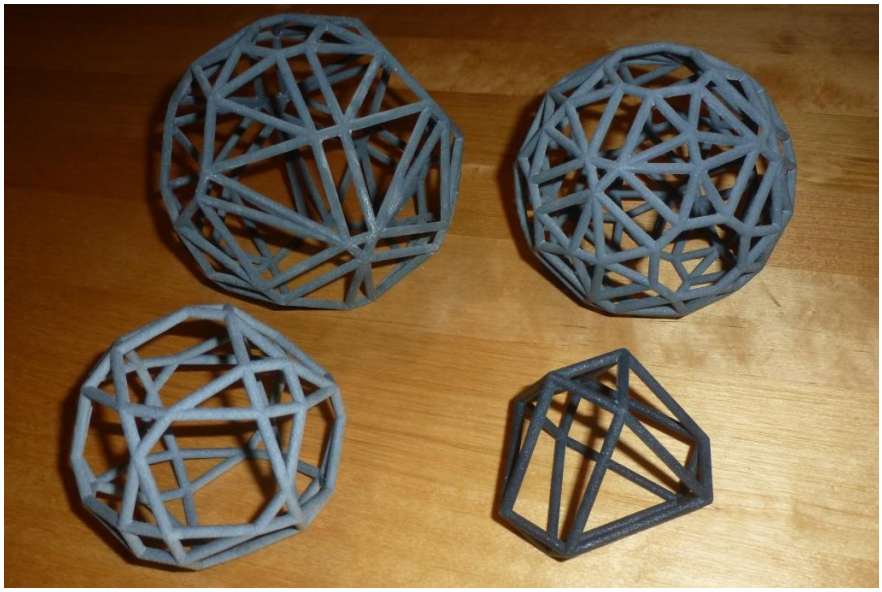

Figure 10: Finished models for $d = 194$ and 41 [back], and $d = 17$ and 19 [front]

4 The Puzzle

4.1 The Idea

If we take one of our polytopes that represents one tessellation, then we can directly compare it to a tessellation using the same subgroup by another method found by Dan Yasaki [7]. This in theory should hopefully give us a way of decomposing our shape into smaller polytopes that we can use to create a puzzle. For the puzzle to be satisfying but challenging we wanted to find a way to get the pieces to connect such that you knew if they were correctly fitted and for it to be not too complicated with loads of components.

4.2 Comparing the tessellations

First we define cross ratio of four distinct points to be,

$$(z_1, z_2 : z_3, z_4) = \frac{(z_1 - z_3)(z_2 - z_4)}{(z_2 - z_3)(z_1 - z_4)} \tag{7}$$

then the dilogarithm function,

$$Li_2(z) = \sum_{k=1}^{\infty} \frac{z^k}{k^2} = z + \frac{z^2}{2^2} + \frac{z^3}{3^2} + ... \tag{8}$$

and the Bloch - Wigner function,

$$D_2(z) = \mathrm{Im}(Li_2(z)) + \mathrm{Arg}(1 - z)\log(|z|),\ z \in \mathbb{C}\backslash[0, \infty) \tag{9}$$

Then the hyperbolic volume of a 3-simplex with vertices on the boundary of $\mathbb{H}^3$ is, $|D_2((z_1, z_2 : z_3, z_4))|$.

The Bloch - Wegner function has the property that,

$$D_2(z) = D_2\left(1 - \frac{1}{z}\right) = D_2\left(\frac{1}{1-z}\right) = -D_2\left(\frac{1}{z}\right) = -D_2(1-z) = -D_2\left(1 - \frac{1}{1-z}\right)$$

so since the six possible values of the cross ratio are: λ, $1 - \frac{1}{\lambda}$, $\frac{1}{1-\lambda}$, $\frac{1}{\lambda}$, $1 - \lambda$ and $1 - \frac{1}{1-\lambda}$, by taking the absolute value it doesn't matter which cross ratio we calculate.

Thus to find the volume of our polytopes we first decompose them into 3-simplexes and apply the Bloch - Wigner function to each component of this triangulation and sum the absolute values.

We use the triangulation in the data for each d and the data calculated independently and separately by Dan Yasaki [8] to compare the volumes of two tessellations for the same d. If we get equal volumes then it suggest we can find a decomposition of our first polytope into smaller Yasaki type one.

4.3 Fitting it all together

The idea for constructing the puzzle is to use spherical magnets that were taken from hobby kits, such as Zen Magnets. These would give us a way of connecting the pieces together at the vertices and hold the pieces in place, while the puzzle was being constructed. I tested combining the 3-d printer and these magnets and the result was very pleasing. However these magnets have a fixed behaviour when more than two come together. This would be a problem around vertices where more than 4 pieces we joining together. To get abound this I employed the use of steel ball bearings that behaved in a better way.

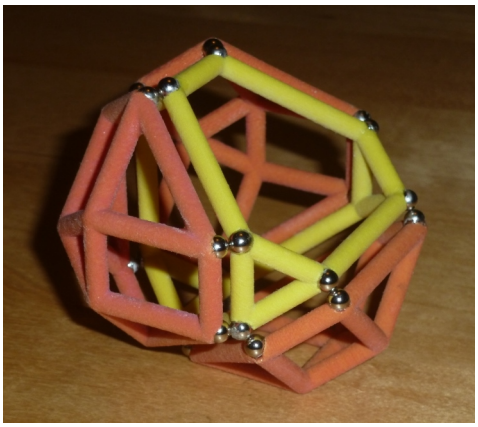

Figure 11: Four pieces for the decomposition $d = 6$ fitted together using only Zen Magnets in the method described above

The initial calculations showed that we could decompose the first polytope corresponding to $d = 6$ into a Truncated Tetrahedron and four Hexagonal Caps. Our hyperbolic volume comes out as:

$$31.0930373... = 7.9183340... + 4 \times 5.7936758...$$

the decomposition values calculated from Yasaki's data [8]. Also for $d = 17$ we can decompose the first polytope into: a Truncated Tetrahedron, four Hexagonal Caps, twelve quadrangle based pyramids and six Triangular Prisms. However these calculations do not tell us how to decompose our shapes into these constituent parts, and it is here that these decompositions become quite arbitrary. Looking at other cases for example $d = 34$ and 57 we can just decompose them in any way that we like however our pieces will not necessarily represent a tessellating polytope of our bigger Hyperbolic Space. Furthermore for this class of polytope ($d = \frac{n^2+2}{3}$) we have two faces that are equilateral triangles side length 2, but with increasing d the radius of the sphere around these shapes increases with $\sqrt{d}$ and as such side lengths of faces of these polytopes are different. This is evident as each of these has the underlying symmetry of the octahedron and

can be decomposed in very similar ways into basis structure containing a Truncated Tetrahedron and four Hexagonal Caps, or a Cuboctahedron. This means that it would be very unlikely to find the pieces from one case could be arranged into the other as initially hoped. Also they are decomposed in a very similar way, so once you understand how one fits together you could make the jump easily to the more complicated cases.

5 Summary

In this project I have managed to calculate a mathematical way of transforming the points generated into nicely symmetric models and have successfully been able to print them. I have found some underlying structure to these polytopes in general and presented my findings here, and since this is in general, infinitely many different models from the same class can be rendered. There is still more work to be done, as I have mostly looked only at the first polytopes for each d, but my method can easily be applied to cases where we don't necessarily have a constant set of fixed points. Additional research could be carried out into the classes of polytopes, and potentially every d could be classified. Furthermore different symmetry groups not mentioned here could be possible.

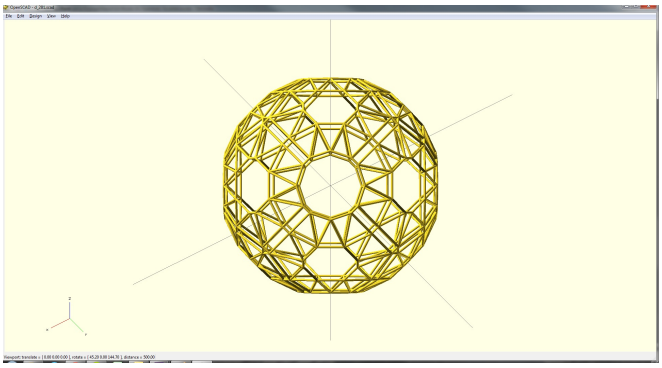

Figure 12: Wireframe model for $d = 281$ [using OpenSCAD] [5]

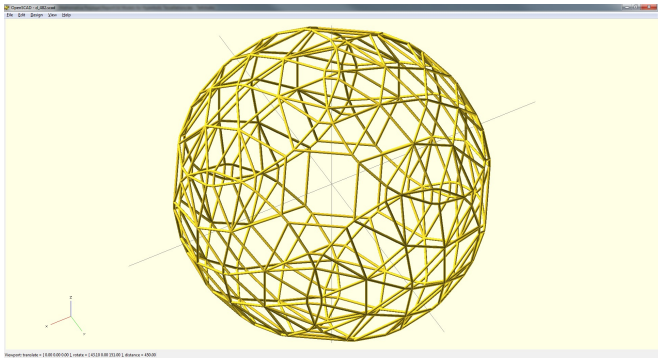

Figure 13: Wireframe model for $d = 482$ [using OpenSCAD] [5]

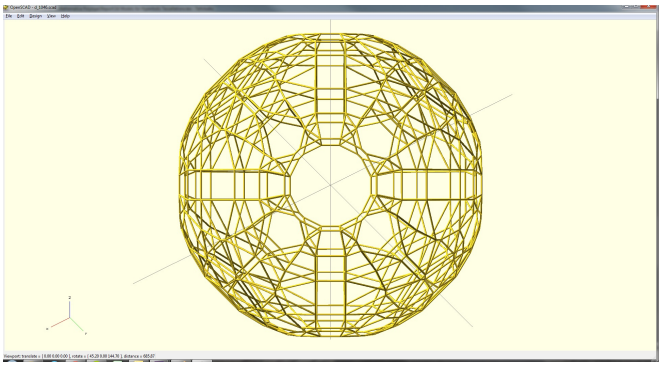

Figure 14: Wireframe model for $d = 1046$ [using OpenSCAD] [5]

References

[1] Herbert Gangl, *Werte von Dedekindschen Zetafunktionen, Dilogarithmuswerte und Pflasterungen des hyperbolischen Raumes.*

http://www.maths.dur.ac.uk/ dma0hg/dipl_thesis.pdf, pp. 20, (1989).

[2] Herbert Gangl, *Tessellations of Hyperbolic space, Notes for an undergraduate colloquium. OCT 2013.*

http://www.maths.dur.ac.uk/ dma0hg/undergrad_colloq_2013.pdf, (2013).

[3] J. Cremona, *Hyperbolic tessellations, modular symbols, and elliptic curves over complex quadratic fields.* Comp. Math. 51, no.3 (1984), pp. 275 - 324.

[4] Mathieu Dutour.

http://mathieudutour.altervista.org/.

[5] OpenSCAD, http://www.openscad.org/.

[6] Chris (Kit) Wallace, *Polyhedra in OpenSCAD.*

http://kitwallace.co.uk/3d/solid-index.xq.

[7] Dan Yasaki, *Hyperbolic Tessellations Associated to Bianchi Groups.* ANTS-IX 2010, LNCS 6197, pp. 385 - 396, (2010).

[8] Dan Yasaki, *Imaginary Quadratic Data.*

http://www.uncg.edu/mat/faculty/d_yasaki/data/imquad-alternating-sum/olddata/.

[9] Mathieu Dutour.

http://mathieudutour.altervista.org/.